Process Safety and Environmental Protection 199 (2025) 107235

Contents lists available at ScienceDirect

Process Safety and Environmental Protection

journal homepage: www.journals.elsevier.com/process-safety-and-environmental-protection

Underground fires induced by disposed Li-ion battery in peatland and landfill

Yuying Chen [a,b], Lei Zhang [a,*], Yichao Zhang [a], Yuxin Zhou [a], Zifan Zhang [a], Shaorun Lin [a], Wei Wei [c], Xinyan Huang [a,**]

[a] Department of Building Environment and Energy Engineering, The Hong Kong Polytechnic University, Hong Kong
[b] The Hong Kong Polytechnic University Shenzhen Research Institute, Shenzhen, China
[c] School of Civil and Environmental Engineering, University of Technology Sydney, Sydney, Australia

ARTICLE INFO

Keywords:
Landfill fire
Waste management
Smoldering ignition
Li-ion battery
Short circuit
Battery thermal runaway

ABSTRACT

Battery-induced fires have become an increasing concern, posing significant environmental and safety risks. This work investigates the smoldering ignition of underground fire in peatland and landfill by disposed Lithium-ion batteries. Both internal and external short circuits of the 18650 cylindrical battery cell are triggered to initiate an in-depth fire of typical landfill soil waste with various moisture contents. Results show that a minimum state of charge (SOC) of 50 % is required for a single-battery thermal runaway to initiate a smoldering fire in the dry waste, which increases with waste moisture. About 18 ± 5 % of battery energy is transferred to the waste within 6–10 min as effective heating for smoldering ignition. For external short circuits, the major ignition source is the Joule heating of the external resistor, not the heating from the battery itself. The propensity of ignition is controlled by both heating intensity and duration, so it varies with the battery SOC and external resistance. A fully charged cell (internal resistance of 35 mΩ) requires a minimum external resistance of 60 mΩ to ignite the dry waste. If the moisture of waste reaches 30 % or above, a single cell cannot initiate a smoldering fire, regardless of external or internal short circuits in current test setups. This work reveals a possible mechanism of landfill fires induced by disposed battery failure and thermal runaway, highlights fire safety issue of disposed batteries, and supports wildfire prevention and suppression strategies for landfills.

1. Introduction

With rapid global urban development and population growth, the quantity of municipal solid waste (MSW) produced worldwide keeps increasing significantly (Liamsanguan and Gheewala, 2008). By 2025, the annual global MSW production is expected to exceed two billion tons (Makarichi et al., 2018). Fires in the MSW management process have occurred frequently in recent years (see Fig. 1a), drawing growing attention. In particular, as the discarded Lithium-ion batteries (Li-ion batteries or LIBs) flood waste streams, the number of waste fires increase sharply, posing an unexpected challenge to the waste industry.

Sanitary landfilling or open dumping remains one of the most common methods for disposing of MSW due to its low cost and minimal technical requirement (Masalegooyan et al., 2022). For example, in America, approximately 53 % of MSW is discarded in landfills; and in China, over 70 % of MSW is treated through landfilling (Dabrowska et al., 2023). Regarding the disposed LIBs, it was reported that only about 5 % are recycled because of the complex and costly process, and the remainder often ends up in landfills (Zhao et al., 2024). The presence of disposed LIBs in landfills will increase the fire risks. For example, in 2021, a landfill fire was caused by the spontaneous combustion of Li-ion batteries in the suburb of Sydney (SARET Research Team, 2023). In July 2023, a laptop was found emitting smoke on the active face of the Hartland Landfill in British Columbia (Saanich News Staff, 2023).

Fire incidents are common among all the landfills worldwide. For instance, the United States has experienced around 2.56×10^{-5} landfill fires per million inhabitants annually (Eurostat et al., 2015). Landfill fires are generally categorized as surface fires and underground fires (Milosevic et al., 2018). Surface landfill fires usually involve the flaming of waste on or close to the surface, whereas underground landfill fires occur deeper and can smolder in-depth for days, months, or even years (Chrysikou et al., 2008; Dabrowska et al., 2023). Smoldering fire is characterized by its slow, low-temperature, and flameless nature, which

* Correspondence to: ZN808, 181 Chatham Road South, Kowloon, Hong Kong.
** Correspondence to: ZS832, 181 Chatham Road South, Kowloon, Hong Kong.
E-mail addresses: lei23.zhang@connect.polyu.hk (L. Zhang), xy.huang@polyu.edu.hk (X. Huang).

https://doi.org/10.1016/j.psep.2025.107235
Received 19 March 2025; Received in revised form 15 April 2025; Accepted 29 April 2025
Available online 1 May 2025

Nomenclature

Symbols

A	cross-section area of the wire (m^2)
cp	specific heat capacity (J/g-K)
C	battery capacity (mAh)
E	energy (kJ)
E''	energy release rate (kJ/s)
ESC	external short-circuit
I	current (A)
ISC	internal short-circuit
L	length of the wire (m)
LIB	lithium-ion battery
m	mass (g)
MC	moisture content (%)
PTC	positive temperature coefficient
Q	Energy (kJ)
R	resistance (mΩ)
S	surface area (m^2)
SOC	state of charge
t	time (s)
T	temperature (°C)
TC	thermocouple
U	voltage (V)

Greeks

ρ	density (kg/m^3)

Subscripts

esc	external short-circuit
isc	internal short-circuit
max	maximum

is one of the most persistent types of combustion phenomena (Rein, 2013). Smoldering peatland and coal mine fires can burn underground for months and years, despite extensive rains, weather changes, or fire-fighting attempts (Lin et al., 2021, 2020; Qin et al., 2022; Song et al., 2020).

The uncontrolled fires in landfills may be triggered by multiple causes, like sparks from machinery being operated in the landfill, intentional arson, lightning strikes, discarded cigarettes, battery thermal runaway, or even spontaneous combustion (Øygard et al., 2004). Spontaneous combustion and arson are identified as the two primary causes, but the cause of many of these fires remains unknown, as shown in Fig. 1(b). Many underground landfill fires could hibernate in deep layers for months. When the dry season comes, these smoldering landfill fires will spread upward and trigger a flame on the surface, which looks like a new fire or a spontaneous ignition (or self-ignition) (Huang and Rein, 2019; Scholten et al., 2021; Zhang et al., 2024b). Additionally, the methane released from waste anaerobic decomposition can lead to uncontrolled gas migration in the absence of an effective gas collection system, which may cause a severe fire and explosion hazard when the level of methane reaches its explosion concentration (Milosevic et al., 2018; Mor and Ravindra, 2023; Themelis and Ulloa, 2007).

Landfill fires pose serious risks to human health, natural environment, and the economy. Since landfill sites contain complex wastes, sometimes with some hazardous materials inside, their burning will release toxic pollutants into the atmosphere, such as dioxin, greenhouse gases (GHG), carbon monoxide (CO), nitrogen oxides (NO_x), black

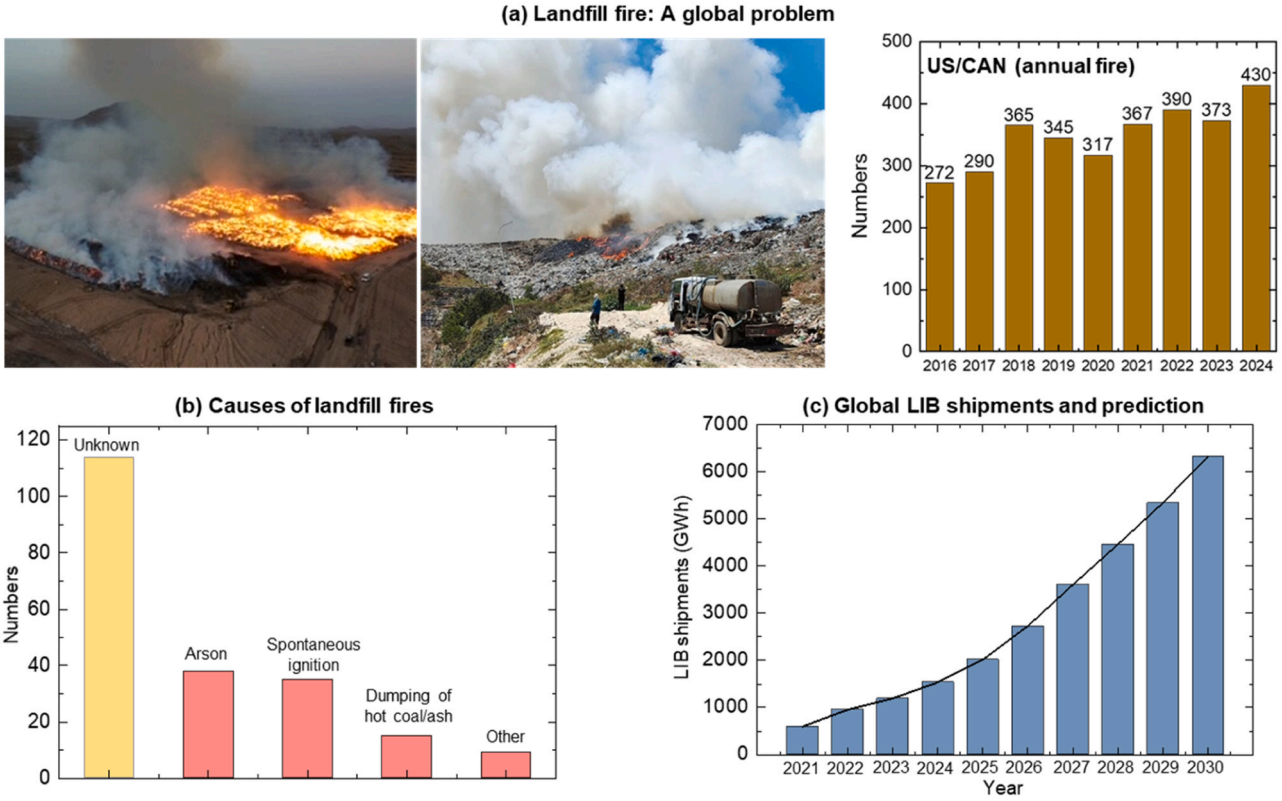

Fig. 1. (a) Typical landfill fire and annual reported waste & recycling facility fires in US/CAN from 2016 to 2024 (adapted from https://www.waste360.com), (b) causes of landfill fires in New South Wales, Australia reported by EPA (Fattal et al., 2016), and (c) global annual LIB shipment and prediction.

carbon (BC), and particulate matters (PMs) (Bihałowicz et al., 2021; Chrysikou et al., 2008; Seidelt et al., 2006; Weichenthal et al., 2015). These emissions can contaminate the surrounding environment and ultimately pose severe health hazards to living organisms (Bihałowicz et al., 2021). In addition, landfill fires can directly threaten human lives, as demonstrated by the 2005 spontaneous landfill fire in Indonesia, which caused the collapse of the waste mountain, killing 140 + people (Koelsch et al., 2005). However, the issue of landfill fires remains poorly understood, with limited information on their causes, frequency, and impacts. Therefore, there is a growing need to address landfill fires and develop effective mitigation strategies for future severe landfill fires.

Li-ion batteries (LIBs) have been more and more widely used in various electronic devices and electric vehicles (EVs) (see Fig. 1c) because of their high energy density, low memory effect, and environmental benefits (Wang et al., 2012, 2023). LIBs may fall into thermal runaway easily because of their flammable compositions and high energy density, which usually occurs with smoke, fire, or explosion (Zhu et al., 2023). In 2021, more than 3000 EV fires in China were attributed to LIB thermal runaway, causing severe loss of life and property (Hu et al., 2021).

The failure and thermal runaway of LIBs could be triggered by various kinds of abuse, including mechanical, electrical, and thermal abuse (Feng et al., 2020; Liu et al., 2022). Most failure modes involve a short circuit, which is an event where the cathode and anode are connected by a low-resistance path, resulting in high current and rapid heat generation (Abaza et al., 2018). Generally, short circuits can occur internally or externally. Internal short circuits (ISC) occur when the insulating separator between the electrodes fails (Maleki and Howard, 2009). This failure mode is reported to account for more than 50 % of fire accidents in electrical vehicles (Li et al., 2024). In practice, the nail penetration test simulates the ISC of LIBs, where a nail punctures the separator and connects the positive and negative current collectors (Gabbar et al., 2021). External short circuit (ESC) occurs when the tabs are connected via an external resistance, providing a current path that is similar to normal discharge process (Ji et al., 2021).

In recent years, battery-related fire and explosion incidents in waste disposals have increased, threatening the entire waste management sector in many countries (Terazono et al., 2024). Existing literature has indicated that fire incidents in waste treatment facilities are primarily caused by LIBs (Terazono et al., 2024). If LIB thermal runaway occurs in the landfills, the intensive energy released is likely to ignite the surrounding combustible waste, leading to more severe landfill fires. However, research on LIB-induced landfill fires is still very limited, posing a significant research gap.

This work aims to investigate the susceptibility of landfill fires triggered by the LIB thermal runaway, being induced through internal and external short circuits. Organic peat soil was selected to simulate the organic wastes in landfills, due to its high organic content and partial degradation properties (Chen et al., 2023). Commercial 18650 battery cells at various states of charge (SOCs) ranging from 20 % to 100 % were used in the experiments. The ignition thresholds for waste with different moisture contents (MCs) are quantified for batteries under both internal and external short circuits to provide a full picture of landfill fires associated with disposed batteries. This study highlights the importance of the proper recycling of disposed LIBs and electronic devices from the perspective of fire risks.

2. Experimental methods

2.1. Simulated landfill

The organic soil (peat) was selected as the replacement of organic solid waste in landfills as they were similar in some physical and chemical properties, like the high organic contents and partial degradation properties (Chen et al., 2022b). The organic peat soil used in this work had a high organic content of ~97 % and uniform particle size, ensuring good repeatability of the experiments as demonstrated in our previous works (Chen et al., 2023; Zhang et al., 2024b). Before the experiment, the peat sample was thoroughly dried in an oven at 90 ℃ for 48 h and then stored in a sealed box to avoid the re-absorption of the ambient moisture. The moisture content (MC) of the oven-dried peat was tested via a moisture tester, which showed an average value of 2.8 % (on the dry mass basis). The bulk density of the dry peat was measured as 145 kg/m^3 and the porosity of it was 0.90, considering a solid density of 1500 kg/m^3. The elemental analysis for the peat organic matter showed 44.2, 6.1, 49.1, 0.5, and 0.1 % mass fractions for C, H, O, N, and S, respectively.

Generally, the newly placed waste in landfills has an initial moisture content of 25 % (by mass) and will change according to the resultant annual water balance (Krause et al., 2023). Herein, to reflect a more actual situation and show how moisture content affects the ignition susceptibility of landfill waste exposed to LIB thermal runaway, soil moisture contents varying from 2.8 % (oven-dried peat) to 30 % were investigated.

2.2. Li-ion battery

The commercial 18650 NCA LIB cells (INR18650–35E, Samsung SDI Co., Ltd., 3.5 Ah) were selected in this work. The cathode material of both cell formats is made from Lithium Nickel Cobalt Aluminum Oxide ($LiNi_{0.8}Co_{0.15}Al_{0.05}O_2$) and the anode material is intercalation graphite (Lammer et al., 2017). Before the experiment, the SOC of cell was calibrated using a battery cycler (CT-4008T-5V12A, Neware Electronic Co., Ltd). The charging and discharging process of 18650 LIBs was as follows: firstly, the cells were discharged to 2.65 V (0 % SOC) at a constant current of 700 mA and left for 2 h. Then the cells were charged to 4.2 V (100 % SOC) by constant current and constant voltage (CC–CV) mode and left for 1 h. Finally, all cells were discharged to the prescribed SOCs based on their capacity and rested for 3 h.

The thermal runaway of an 18650 cell induced by nail penetration only occurred when SOC was above 30 % (Zhang et al., 2024a). Thus, five SOC levels (>30 %) of 18650 cell were selected for the nail-penetration tests (internal short circuit), i.e., 40 %, 50 %, 70 %, 90 %, and 100 %. Five SOC levels (20 %, 40 %, 60 %, 80 %, and 100 %) were chosen for the battery external short-circuit tests.

2.3. Experimental setup

As shown in Fig. 2, the waste was filled into a top-open tubular steel reactor with a height of 13 cm and an inner diameter of 15 cm. Such cylindrical reactors were widely used in the past smoldering experiments (Chen et al., 2023, 2022a). A 2 cm-thick ceramic insulation layer was attached to the wall of the reactor to reduce the radial heat loss. For each test, one 18650 cell was positioned along the axis of the reactor near the bottom to heat the landfill sample. During tests, the ambient temperature was 28 ± 2 ℃; relative humidity was 50 ± 10 %; and the pressure was 1 atm.

In this work, two methods were employed to trigger the thermal runaway of the battery. That is, the internal short-circuit was induced by a nail penetration system, and the external short-circuit was induced by connecting the cathode and anode with a copper wire. These two methods will be introduced in detail in the following sub-sections. For both experimental systems, a K-type thermocouple (TC) was employed to measure the LIB temperature (T_{LIB}) which was positioned in the middle of the cell. The entire experimental process was captured by a digital camera from the side view, and another IR camera to monitor the surface temperature of the simulated landfill from the top view.

2.4. Internal short-circuit test via nail penetration

A specially designed vertical battery nail penetration system was used to trigger the battery internal short circuit and the following

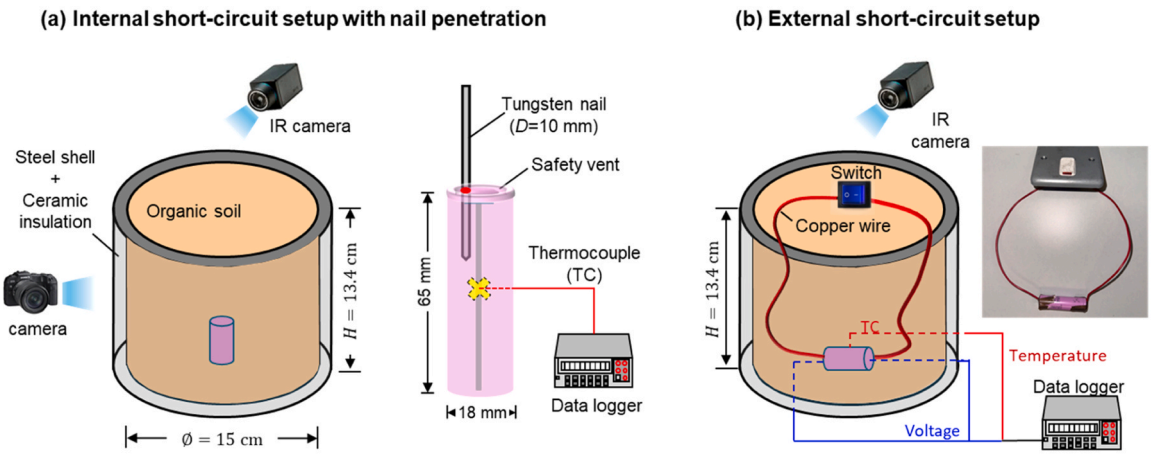

Fig. 2. Schematics of (a) internal short-circuit setup with nail penetration to trigger battery thermal runaway, and (b) external short-circuit setup.

thermal runaway, as shown in Fig. 2(a). The nail employed here was made of tungsten steel and had a length of 200 mm and a diameter of 10 mm. Before the penetration, the cell was vertically fixed with the anode at the top and the cathode at the bottom of the smoldering burner. The penetration direction was parallel to the electrode layers of the cell, and the penetration point was at the surface of the cell's anode. The system was remotely controlled by the computer, and the nail penetration speed of 10 mm/s was selected for all cases to ensure experimental repeatability.

Before each test, the cell was first fixed on the sample holder at the bottom of the smoldering burner. Then, the waste was filled into the burner. Afterwards, the nail height was adjusted to the same position for all cases. A certain distance was reserved between the nail and the cell to guarantee that the penetration speed was stable before contacting the cell. The nail penetration system was activated together with the data acquisition system and video monitoring system. After a full penetration, the nail stayed inside the cell to avoid disturbance to the battery thermal runaway process, and after 5 min, the nail was slowly removed from the battery and soil, controlled by a program, to ensure a safe test process.

2.5. External short-circuit test with resistance wire

The external short-circuit system is shown in Fig. 2(b), where an 18650 cell was connected with a switch and a copper wire. The external resistance of the circuit (R_{ex}) was the sum of the resistance of the wires, switch, and contact resistances, where the latter two were much smaller. Thus, the external resistance of the short circuit was estimated as

$$R_{ex} \approx \frac{\rho L}{A} \tag{1}$$

where $\rho = 1.756 \times 10^{-8}$ Ω·m is the resistivity of the copper, L is the length of the wire, and A is the cross-section area of the wire. Thus, the total resistance of the whole circuit is

$$R_{tot} = R_{LIB} + R_{ex} \tag{2}$$

where R_{LIB} is the initial internal resistance of the LIB, which is around 35 mΩ of an 18650 cell (Zhang et al., 2024a); and R_{ex} can be adjusted by changing the length and cross-section area of the wires. Thus, the discharge speed (i.e., Joule heat release rate) of the external short-circuit of LIBs could be controlled. In this work, five different external resistances (R_{ex}) were selected and measured, that is, 20, 50, 70, 80, and 100 mΩ.

Before each test, the battery cell and copper wires (with PVC coating) were connected by welding, while the switch and the wires were connected by screw. Afterwards, the well-connected circuit (with the switch turned off) was placed into the burner with the battery at the bottom and the switch at the open top. Then, the waste was filled into the burner, and the battery and wires were buried. Finally, the switch was turned on together with the data acquisition system and video monitoring system.

The test was considered finished when all thermocouple measurements of soil and battery dropped to room temperature. The residual waste and battery samples were disposed through standard procedures to minimize the environmental impact. For each test condition, 3–5 repeating tests were conducted to ensure the repeatability and reliability of experimental outcomes.

3. Results and discussion

3.1. Landfill ignition induced by battery thermal runaway

3.1.1. Thermal runaway and ignition phenomenon

The experimental outcome of landfill ignition by the battery internal short circuit (or thermal runaway) is classified into two categories: (a) successful smoldering fire ignition and (b) unsuccessful smoldering ignition. Successful smoldering ignition is defined as the condition where the smoldering can be successfully initiated and become self-sustained, after the heating from the battery thermal runaway. The self-sustained smoldering is evidenced by the surface temperature of the waste bed, captured by the IR camera, and the strong visible smoke.

Fig. 3(a) shows an example of successful smoldering ignition of the dry waste induced by the thermal runaway of a 50 % SOC cell (see supplementary Video S1). The start time (0 s) indicated the moment when the moving nail tip touched the cell. Right after that, a large amount of white smoke was emitted from the battery sharply, indicating the thermal runaway of the battery cell was triggered. After around 5 min, the nail was automatically extracted according to the program, while the battery cell stayed inside the soil. Afterwards, some white smoke was again emitted from the waste smoldering, demonstrating that a stable self-sustaining smoldering was initiated. Additionally, the infrared images of the fuel bed top at 30 min also proved the successful smoldering ignition of the waste.

Supplementary material related to this article can be found online at doi:10.1016/j.psep.2025.107235.

However, the smoldering ignition of moist waste was much more difficult to initiate even under a more intensive battery thermal runaway, as shown in Fig. 3(b) (see Video S2). For the thermal runaway of a 100 % SOC cell, ejecting sparks were generated at about 1 s followed by a strong jet flame. The strong jet flame lasted for several seconds and then transferred to weak diffusion flame, which could last for about 20 s. After the flame extinction, a small amount of smoke was continuously released for a while. After the nail extraction at around

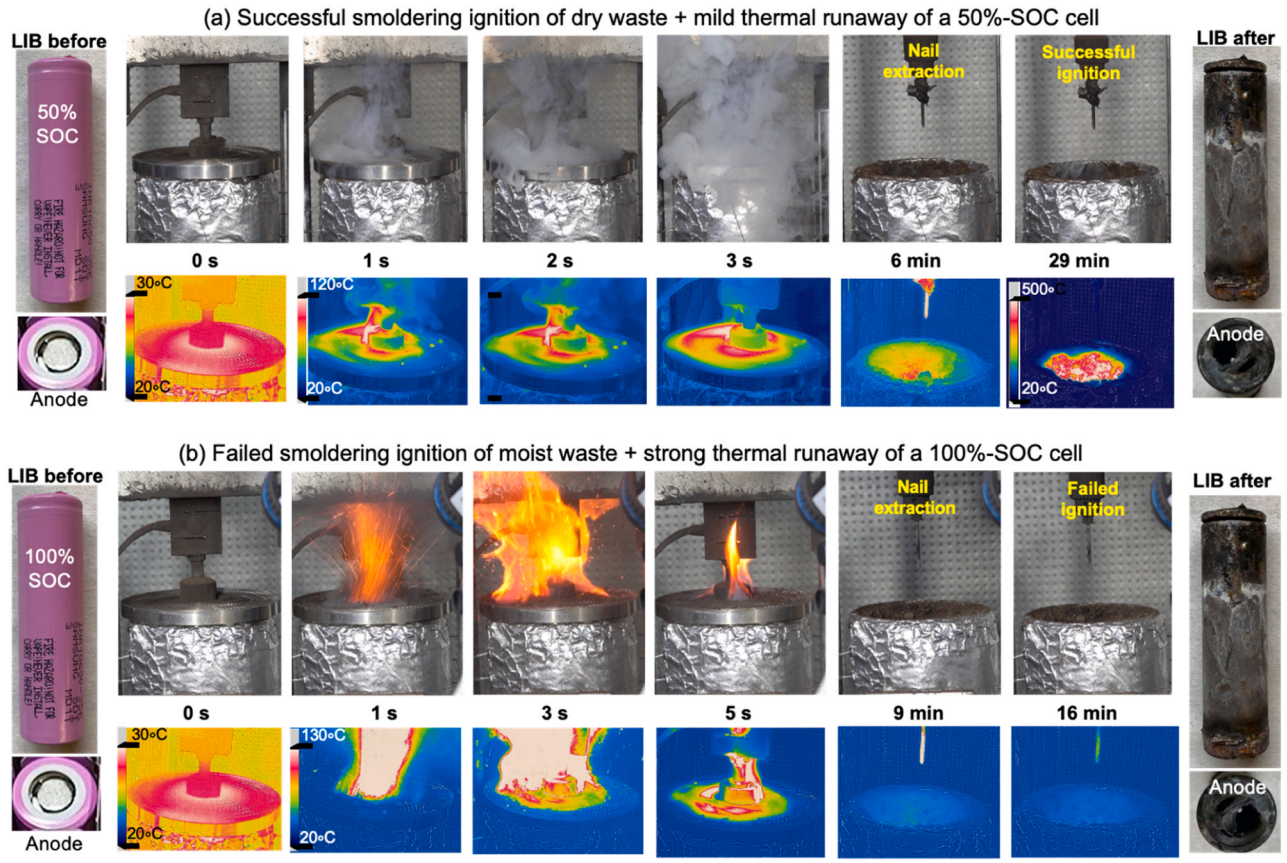

Fig. 3. Experimental phenomena of (a) successful smoldering ignition of dry waste induced by mild thermal runaway of a 50 %-SOC cell (see Video S1) and (b) unsuccessful smoldering ignition of 30 %-MC waste exposed to the strong thermal runaway of a 100 %-SOC cell (see Video S2).

9 min, we can observe no smoke was further generated, indicating an unsuccessful smoldering ignition of the waste. The infrared images in Fig. 3(b) also verified the unsuccessful ignition of the waste. This is because more heat (energy) generation is required for the water evaporation of the moist waste.

Supplementary material related to this article can be found online at doi:10.1016/j.psep.2025.107235.

3.1.2. Thermal impact of battery thermal runaway

Fig. 4(a) shows the evolution of the surface temperature of LIBs (T_{LIB}) with various SOCs ranging from 40 % to 100 % when a nail penetrates through the cells. T_{LIB} increases with the increasing SOC, leading to a more rapid and intense thermal runaway event. For all SOCs, the thermal-runaway duration generally lasts for 30–40 s, after which the cell temperature drops gradually. Fig. 4(b) illustrates that the maximum battery temperature ($T_{LIB,max}$) rises with the SOC. For example, $T_{LIB,max}$ of a 50 % SOC cell is 550 °C and increases to 732 °C when the SOC increases to 100 %.

Fig. 4(c) shows the duration when T_{LIB} exceeds 250 °C ($\Delta t_{250°C}$), extracted from the temperature-evolution curves in Fig. 4(a). The parameter $\Delta t_{250°C}$ is important in characterizing the effective heating time of the cell on the surrounding soil, as 250 °C is the minimum temperature required to initiate a smoldering soil fire (Lin and Huang, 2021). When the battery cell is lower than 250 °C, it may become a cooling source to the smoldering ignition process of waste. As demonstrated, the $\Delta t_{250°C}$ of the thermal runaway of a 50 % SOC cell is around 356 s (~ 6 min), while this value increases to 610 s (~10 min) when the SOC increases to 100 %. This means the thermal runaway of cells with a higher SOC will lead to larger heating intensity and longer heating time on the surrounding waste.

3.1.3. Ignition threshold of thermal runaway

Fig. 4(d) summarizes the limiting conditions of smoldering ignition of the waste with different moisture contents up to 30 % induced by the internal short circuit of a cell with various SOCs, where the red solid symbols (●) denote the successful smoldering ignition and the black cross symbols (×) indicate the unsuccessful ignition. In particular, the semi-hollow red symbols represent the probability of successful smoldering ignition between 0 and 1. For example, when using the 90 % SOC cell to ignition the waste with a moisture content of 15 %, one out of three tests showed successful ignition while the remaining two tests failed.

As depicted in Fig. 4(d), when the SOC is lower 50 %, no thermal runaway occurs (as the blue region shows). When the thermal runaway is successfully triggered (i.e., SOC $\geq$ 50 %), the minimum SOC required to trigger a successful smoldering fire increases with the fuel moisture content. For instance, the minimum SOC for igniting dry waste is 50 %, meaning that the self-sustaining smoldering of dry waste will be initiated as long as the battery thermal runaway occurs. As the moisture content of waste increases to 15 %, the minimum SOC required to ignite the smoldering fire increases to 90 %, which is almost two times that for dry waste. However, when the moisture content reaches 30 %, the waste cannot be ignited, even by the thermal runaway of a 100 % SOC cell.

The major portion of heat released from battery thermal runaway stays inside the battery to heat the cell to a peak temperature within 60 s, while a small portion is released via ejected hot emission gases and solid particles. Both the hot battery cell and emission gases will heat the landfill soil. For simplicity, the total thermal-runaway energy stayed inside the battery cell is roughly

$$E_{isc} \approx mc_p(T_{max} - T_a) \quad (3)$$

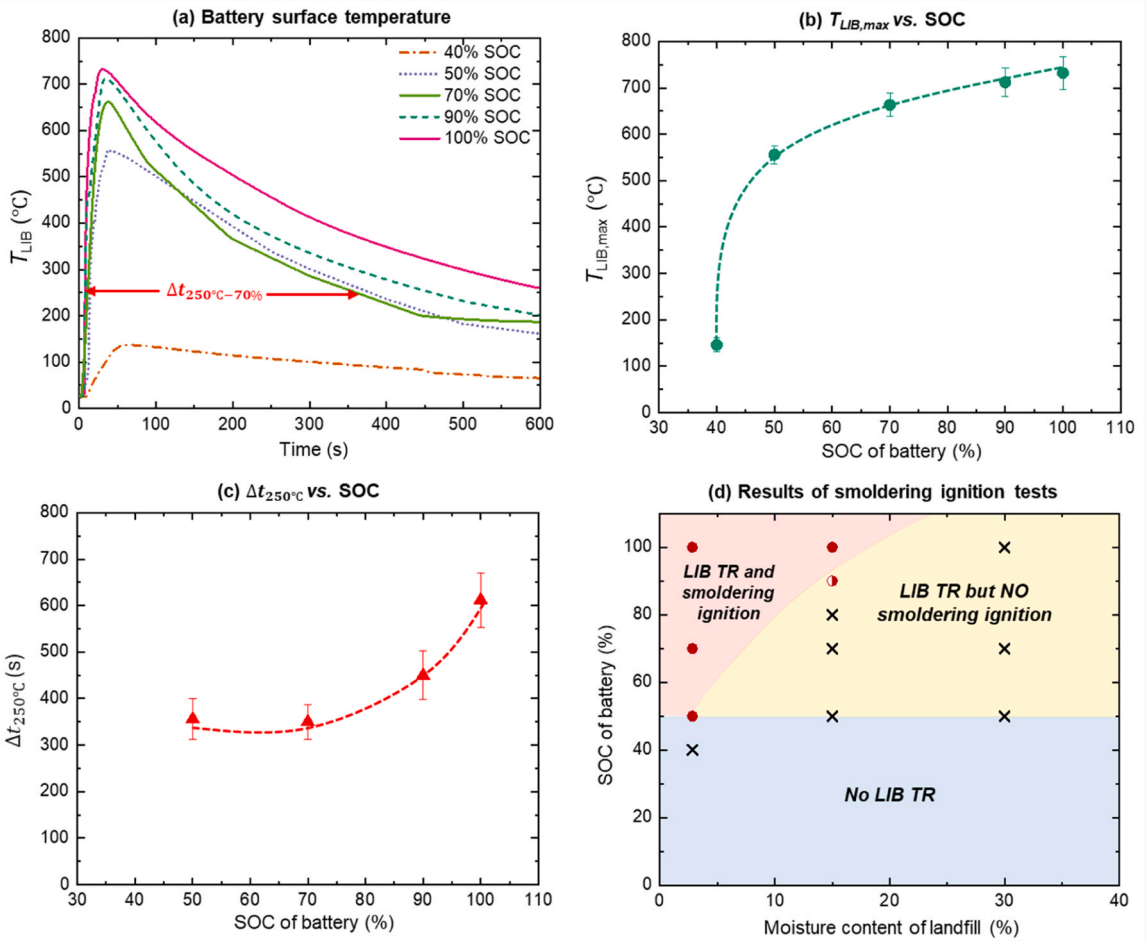

Fig. 4. (a) Evolution of battery surface temperature after the nail penetration, (b) maximum battery temperature ($T_{LIB,max}$), (c) duration when T_{LIB} above 250 °C ($\Delta t_{250°C}$), and (d) summaries of limiting conditions of smoldering ignition induced by battery internal short circuits.

where $m = 48.0$ g is the mass of the battery; $c_p = 1.1$ J/g-K is the specific heat of 18650 cell (Feng et al., 2016); T_{max} is the maximum battery surface temperature; and $T_a = 28$ °C is the ambient temperature. Nevertheless, not all battery energy is effective in igniting the smoldering of soil. The effective heat from the hot battery to the soil for smoldering ignition can be estimated as

$$Q_{ig,isc} \approx \int \dot{q}'' dt = \int hS(T_{LIB} - T_{s,\min})dt \quad (4)$$

where $h \approx 20$ W/m^2-K is the heat transfer coefficient of the cylindrical battery cell (Liu et al., 2024, 2020), $S = 3.67 \times 10^{-3}$ m^2 is the surface area of the cylindrical cell, $T_{s,\min} \approx 250$ °C is the minimum temperature to initiate smoldering soil fire (Lin and Huang, 2021), and T_{LIB} here is the surface temperature of the cell where it is larger than 250 °C.

The stored electric energy of a battery cell is calculated as (Lyon and Walters, 2016)

$$E_{LIB} = C_{LIB} \times SOC \times U_{LIB} \times 3600 \quad (5)$$

where C_{LIB} is the capacity of the battery, mAh, and U_{LIB} is the voltage of a cell at a given SOC, V.

Table 1 summarizes the calculated energy released from LIB internal short-circuit (E_{isc}), the effective ignition heat ($Q_{ig,isc}$), and the battery electric energy (E_{LIB}).

Fig. 5(a) shows a 50 % SOC cell stores 23.3 kJ of electric energy, while it could generate 27.9 kJ of heat from its thermal runaway. This is because some chemical energy is also released from exothermic reactions inside the cell when its thermal runaway occurs. However, only 3.9 kJ is effective in heating the surrounding waste. When the SOC increases to 100 %, the electric energy, the total thermal-runaway energy, and the effective heating energy rise to 53.2, 37.2 kJ and 8.3 kJ, respectively. Moreover, we found the calculated thermal runaway energy is lower than the electric energy at higher SOCs. As heavy smoke (or even flame and sparks) is generated in the thermal runaway of high-SOC cells, hot smoke will take away lots of energy, leading to an underestimation of E_{isc} via Eq. (3).

Table 1
Summary and comparison of E_{isc}, E_{LIB}, and $Q_{ig,isc}$.

SOC (%)	E_{isc} (kJ)	E_{LIB} (kJ)	$Q_{ig,isc}$ (kJ)
40	6.2	18.1	-
50	27.9	23.3	3.9
70	33.5	33.5	4.1
90	36.1	45.4	5.7
100	37.2	53.2	8.3

More importantly, it can be concluded from Fig. 5(a) that the minimum energy required for igniting the smoldering of dry waste in this work is around 3.9 kJ (at 50 % SOC), while the smoldering of moist waste (with the MC of 15 %) requires at least 5.7 kJ energy (at 90 % SOC). However, when the moisture content reaches 30 %, the maximum effective ignition heat from a single cylindrical cell thermal runaway (i.e., 8.3 kJ at 100 % SOC) is not sufficient to ignite the self-sustaining smoldering of waste. Fig. 5(b) shows the heating efficiency (i.e., $Q_{ig,isc}/E_{isc}$ and $Q_{ig,isc}/E_{LIB}$) of the hot cell on surrounding waste. It is found that both ratios are about 18 ± 5 % for all SOCs. In short,

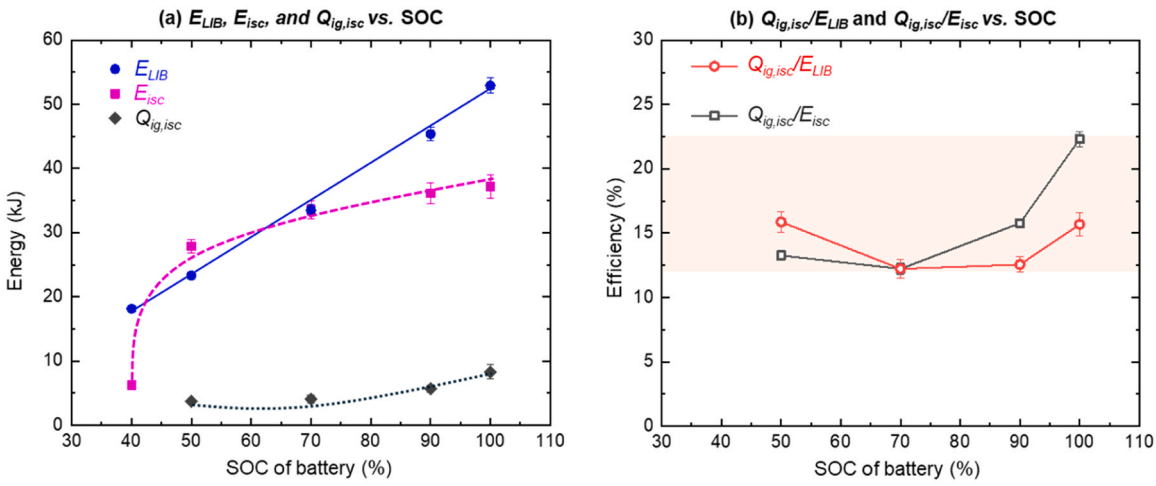

Fig. 5. (a) Battery electrical energy (E_{LIB}), total thermal-runaway energy (E_{isc}), and effective ignition energy ($Q_{ig,isc}$), and (b) heating efficiency of battery on waste.

although the battery thermal runaway generates intensive energy, only a small portion of battery energy is transferred to waste as the effective heating for smoldering ignition.

3.2. Smoldering fire induced by external short-circuit heating

3.2.1. Heating and burning processes

Fig. 6 shows a successful smoldering ignition in dry waste induced by the external short-circuit of a cell (see Video S3). For the case shown here, the SOC of the cell is 80 % and the external resistance of the circuit is around 80 mΩ. Notably, the phenomena of smoldering ignition triggered by battery internal (nail penetration) and external short-circuit are quite distinct. We found that the waste was ignited mainly by the heat released from the wire (external resistor) instead of the cell itself.

Supplementary material related to this article can be found online at doi:10.1016/j.psep.2025.107235.

After the switch-on of the circuit at 0 s, some white smoke was generated subsequently at around 30 s. This smoke was caused by the pyrolysis of the coat of the electrical wire (i.e., PVC). At around 4 min, a small charring region was formed at the surface of the peat bed near the wire; meanwhile, some smoke was released from the waste smoldering. This phenomenon proved that the smoldering of waste was ignited majorly by the Joule heat from the connected wire. Afterwards, the smoldering became more intensive, and the charring region became larger. As shown in the infrared pictures of Fig. 6, the smoldering almost spreads to the whole waste surface at around 70 min. For the phenomenon of the unsuccessful smoldering ignition, generally, no smoke was emitted from the waste, and no charring area was formed in the waste.

3.2.2. Battery temperature, voltage, and current

Fig. 7 shows the evolution of battery surface temperature (T_{LIB}) and voltage (U_{LIB}), and the calculated shorting current (I_{short}) after its external short-circuit is triggered, where $I_{short}=U_{LIB}/R_{ex}$. It can be found that the voltage and current will drop to zero once the LIB temperature reaches its peak for all the tested conditions. This is because the Current Interrupt Device (CID) inside the battery is activated at such a moment, causing the break of the circuit. The commercial cylindrical 18650 cells typically have a CID device installed into the cell cap to disconnect the internal electrical circuit when abnormal conditions are detected, like the temperature or pressure rises above a threshold. Therefore, after the activation of CID, both the voltage and current of the circuit drop to zero and the LIB temperature starts to decrease gradually.

Fig. 7(a) shows the effect of external resistance on the external short circuit of a 100 % SOC cell. As depicted, the maximum battery temperature is comparable across different external resistances at around 140 °C. However, smaller external resistance results in a more rapid temperature rise of the cell and causes an earlier break of the circuit. For example, in the circuit with an external resistance of 20 mΩ, the LIB temperature peaks instantly at around 40 s, with both the voltage and current dropping to zero. Comparatively, for the circuit with an external resistance of 100 mΩ, the LIB temperature peaks later at around 1 min 50 s, with the current of the circuit maintained at 26 A for around 90 s. This is because the CID inside the cell is activated earlier for the circuit with lower external resistance (i.e., larger current).

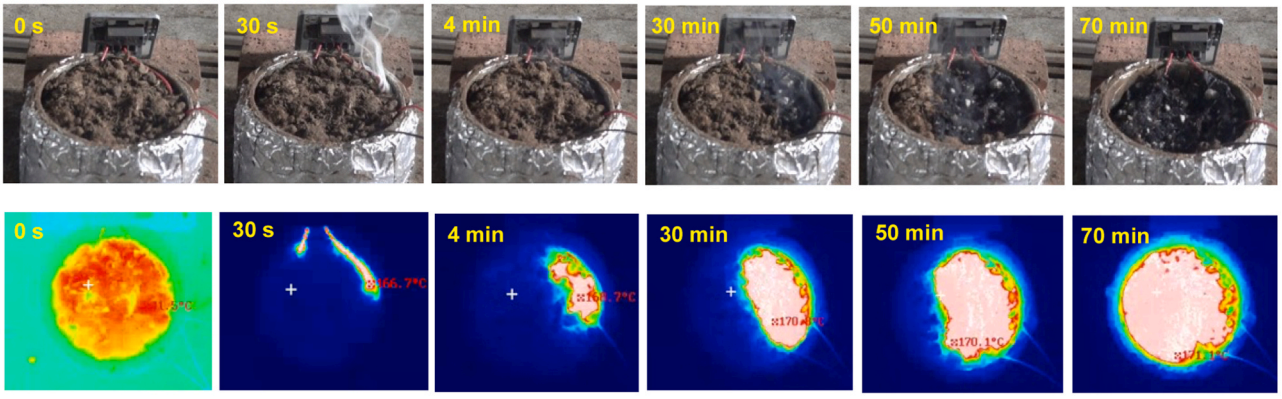

Fig. 6. Successful smoldering ignition of dry waste induced by the external short-circuit of an 80 % SOC cell with an external resistance of 80 mΩ, where the peak temperature of the top surface is marked in the IR image (also see Video S3).

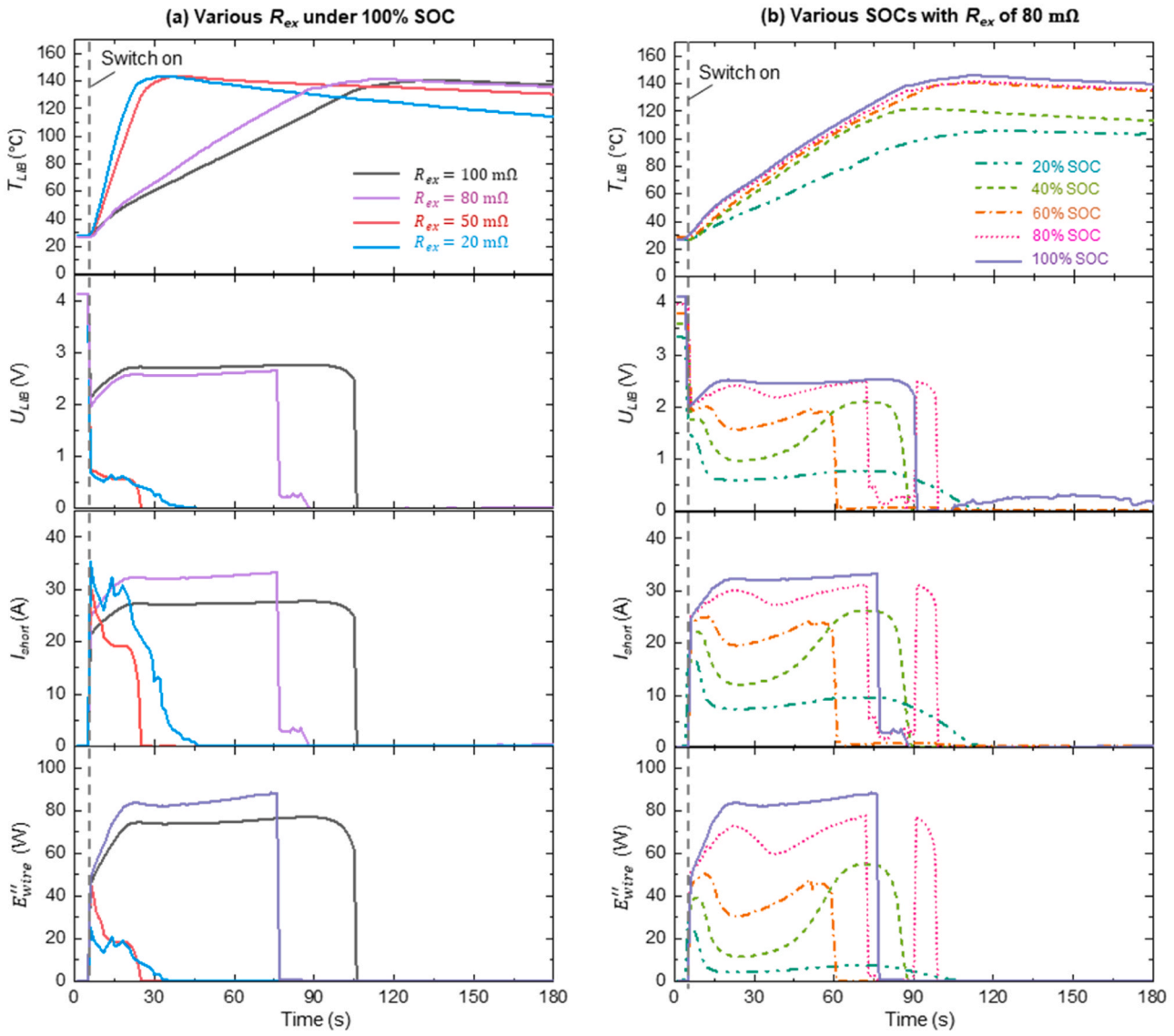

Fig. 7. Evolution of battery surface temperature (T_{LIB}), voltage (U_{LIB}), and current (I_{LIB}) as well as the energy release rate from the connection wire (E''_{wire}) of (a) 100 % SOC cells under various external resistances and (b) cells with various SOCs when the external resistance is fixed at 80 mW.

Fig. 7(b) exhibits the effect of battery SOC on the external short circuit of a cell with a fixed external resistance of 80 mΩ. First, the maximum temperature of the battery increases with the increasing SOC. For example, the peak T_{LIB} increases from 105 °C to 147 °C as the SOC rises from 20 % to 100 %. Second, a higher SOC will lead to a more intensive energy release of the cell with a larger current in the circuit. For example, the maximum current of the external short-circuit of a 20 % SOC cell is around 18 A, while this value increases to 32 A as the SOC increases to 100 %.

3.2.3. *Ignition threshold of Joule heating*

Fig. 8(a-b) summarize the limiting conditions of smoldering ignition induced by the external short-circuit of a cell. Fig. 8(a) shows the relationship between waste moisture content (MC) and external resistance of the circuit (R_{ex}) when the cell SOC is 100 %. For a fully charged cell, its external short-circuit could cause the smoldering ignition of dry waste when its connected external resistance is larger than 60 mΩ. As the waste moisture content increases to 15 %, the minimum external resistance required for the circuit to initiate smoldering increases to 80 mΩ. The circuit with a large external resistance can sustain a slower discharge over an extended period, thereby allowing the circuit to remain at high temperatures longer.

Fig. 8(b) shows the smoldering susceptibility of waste when ignited by the external short-circuit of a cell with various SOCs under an external resistance of 80 mΩ. As expected, the minimum SOC required for igniting the smoldering of waste increases with the fuel moisture content. For example, as the moisture content increases from 3 % to 15 %, the limiting SOC increases from 40 % to 80 %. This is because more energy is required for the water evaporation of the moist waste. However, the waste with 30 % MC cannot be ignited any more by a single cell within the tested range.

Generally, the energy released from the LIB external short circuit includes two parts, the battery and the external resistance. However, as demonstrated in the experimental phenomenon, the waste was ignited by the heat generated by the wires. Therefore, this work considers only the energy (Joule heat) released by the wires as the effective ignition energy for initiating the smoldering of waste, that is

$$Q_{ig,esc} = E_{wire} = \int E''_{wire} dt = \int (I_{wire})^2 R_{wire} dt \quad (6)$$

where I_{wire} is the current passing through the wires which is equal to the I_{short} in Fig. 7, and R_{wire} is the equivalent resistance of the wire. E''_{wire} is the

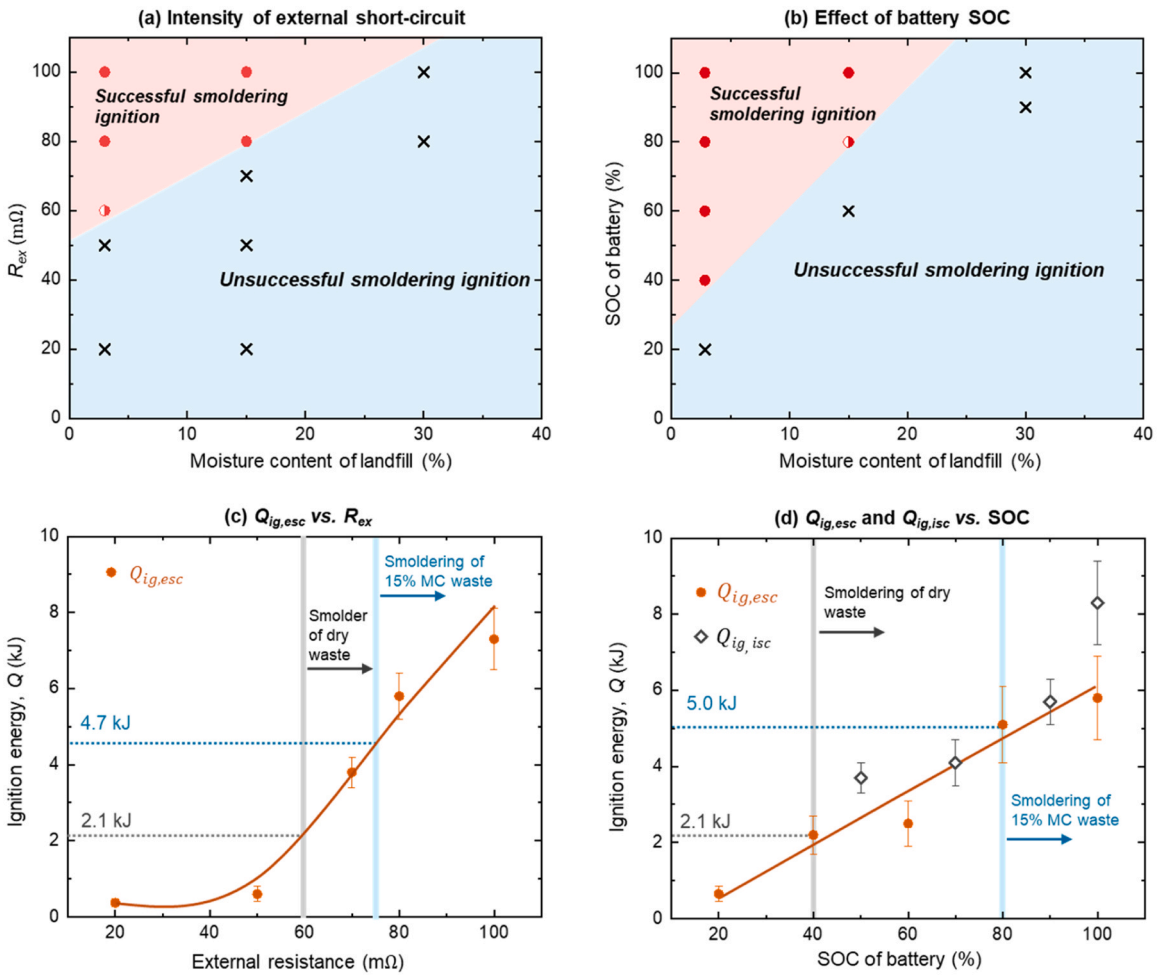

Fig. 8. Effects of (a) external resistance and (b) battery SOC on the limiting conditions of smoldering ignition induced by the external short-circuit of a cell, and the ignition energy from battery external short circuits under (c) various external resistances and (d) different SOCs, where the hollow symbols in (d) indicate the effective ignition energy from battery internal short circuits (by nail penetration).

Joule heat release rate from the wire. The calculated E''_{wire} is shown in the bottom layer of Fig. 7.

Fig. 8(c-d) show the calculated effective ignition energy from the external short-circuit of the cell ($Q_{ig,esc}$). $Q_{ig,esc}$ increases with both the external resistance (R_{ex}) and the SOC of battery. For example, the effective ignition energy from the short-circuit of a 100 % SOC cell increases significantly from 0.4 kJ to 7.3 kJ as the external resistance increases from 20 mΩ to 100 mΩ (see Fig. 8c). Moreover, Fig. 8(d) shows the ignition energy from the external short-circuit of a 20 % SOC is 0.65 kJ when the external resistance is fixed at 80 mΩ. Notably, Fig. 8(c-d) also show the minimum energy required to ignite the dry waste is only 2.1 kJ, while a larger energy of around 5.0 kJ is required for the smoldering ignition of the waste with the moisture content of 15 % regardless of the battery SOC and external resistance. In addition, Fig. 8(d) shows that the estimated effective ignition energy generated from battery internal short-circuit (induced by nail penetration) is slightly smaller than that from external short-circuit under the same SOC in this work.

3.3. Implications

Both the internal and external short circuits of LIBs could lead to the smoldering fire of landfill waste. Internal short circuits (induced by nail penetration) result in intensive and rapid energy release of the battery, which may occur during waste collection and treatment due to mechanical abuse. However, only a small portion of the thermal-runaway energy is effective in heating the surrounding waste. Although external short circuits release energy more slowly and at a lower intensity, they present a higher risk of causing landfill fires, even when the battery SOC is as low as 40 %. Whether the battery's external short circuit can ignite the waste highly depends on the external resistance it connects with; only a relatively larger external resistance can generate sufficient heat to ignite the waste. This suggests that when a disposed battery is accidentally connected by a conductive object in landfills, the formed circuit may easily trigger a landfill fire. In addition, the susceptibility of igniting landfill smoldering fires is extremely sensitive to the waste moisture content. When the moisture content exceeds 30 %, the waste cannot be ignited by the thermal runaway of a single cell. Therefore, the landfill managers and operators should pay more attention to landfill fires during dry seasons and avoid mechanical abuse (like crushing and striking) when handling waste.

This work has only addressed the tip of the iceberg for complex ignition and fire problems in landfills, so many future studies are needed to understand the problem better. For example,

(1) In the nail penetration test, the enormous force generated by battery thermal runaway caused some fuel near the cell to be displaced, which may affect the full contact between the cell and the fuel. Thus, the battery's internal short-circuit test device will be improved in the future to solve this problem.
(2) This work only focused on the short circuits of a single commercial 18650 battery cell. In our future works, the influence of

the battery type, size, and energy density on landfill ignition propensity will also be explored.

(3) In the external short-circuit tests, the connection wires used were PVC-coated, leading part of the heat generated by the wires was used to decompose the PVC coating, rather than heating the soil directly.

(4) This work used peat to represent the organic waste in landfills. However, there are many more types of complex waste compositions in actual landfills, which have different levels of ignitability, moisture content, and fire risk. Thus, future work will also focus on exploring the effect of waste properties on ignition susceptibility.

4. Conclusions

In this work, we investigated the ignition susceptibility of landfill and solid waste (using peat soil as a representative) induced by the internal and external short circuits of commercial 18650 Lithium-ion batteries at various SOCs ranging from 20 % to 100 %. The internal short circuits were triggered by nail penetration. Results showed the thermal runaway of the battery occurred when their SOCs reached 50 % or higher, which released intense energy rapidly within seconds, causing a sharp increase of the battery surface temperature beyond 500 °C. The minimum SOC required for ISC to ignite the smoldering of dry waste was 50 %, while it increased to 90 % for waste with 15 % MC. About 18 % of battery energy is transferred to waste as effective heating for smoldering ignition, and the effective heating time during battery thermal runaway is about 6–10 min.

The external short circuits were triggered by connecting the anode and cathode with a copper wire. External short circuits released energy at a slower rate and lower intensity, with the maximum battery temperature varying from 100 to 145 °C depending on the SOC. The ignition of waste was primarily caused by the heat generated by the external resistor of the circuit rather than the battery itself, which was affected by both the battery SOC and external resistance. A 100 % SOC cell required a minimum external resistance of 60 mΩ to ignite the smoldering of dry waste, while a minimum SOC of 40 % was required for igniting the dry waste when the external resistance was 80 mΩ. However, when the moisture content of the waste reached 30 %, smoldering fire could not be ignited by either external or internal short circuits of a single cylindrical battery under the tested conditions.

This work reveals a possible mechanism of landfill fires induced by disposed battery failure and thermal runaway, highlights fire safety issue of disposed batteries, and supports wildfire prevention and suppression strategies for landfills. Future work shall explore the different types and capacity of batteries and quantify the ignition limits of various wastes under the thermal runaway and external short circuit of these batteries.

CRediT authorship contribution statement

Chen Yuying: Writing – original draft, Resources, Investigation, Formal analysis, Data curation. **Zhang Lei:** Resources, Methodology, Investigation. **Zhang Yichao:** Resources, Formal analysis. **Zhou Yuxin:** Resources, Formal analysis. **Zhang Zifan:** Resources, Formal analysis. **Lin Shaorun:** Resources, Formal analysis. **Wei Wei:** Supervision, Formal analysis. **Huang Xinyan:** Writing – review & editing, Supervision, Funding acquisition, Conceptualization.

Declaration of Competing Interest

The authors declare that they have no known competing financial interests or personal relationships that could have appeared to influence the work reported in this paper.

Acknowledgements

This research is funded by the National Natural Science Foundation of China (No. 52322610), and RGC Hong Kong GRF Scheme (No. 15221523). The authors thank Jiekai Xie and Yanhui Liu (HK PolyU) for their valuable comments.

References

Abaza, A., Ferrari, S., Wong, H.K., Lyness, C., Moore, A., Weaving, J., Blanco-Martin, M., Dashwood, R., Bhagat, R., 2018. Experimental study of internal and external short circuits of commercial automotive pouch lithium-ion cells. J. Energy Storage 16, 211–217. https://doi.org/10.1016/j.est.2018.01.015.

Bihałowicz, J.S., Rogula-Kozłowska, W., Krasuski, A., 2021. Contribution of landfill fires to air pollution–an assessment methodology. Waste Manag. 125, 182–191.

Chen, Y., Lin, S., Liang, Z., Huang, X., 2022a. Clean smoldering biowaste process: effect of burning direction on smoke purification by self-sustained flame. Fuel Process. Technol. 237, 107453. https://doi.org/10.1016/j.fuproc.2022.107453.

Chen, Y., Lin, S., Liang, Z., Surawski, N.C., Huang, X., 2022b. Smouldering organic waste removal technology with smoke emissions cleaned by self-sustained flame. J. Clean. Prod. 362, 132363. https://doi.org/10.1016/j.jclepro.2022.132363.

Chen, Y., Lin, S., Qin, Y., Surawski, N.C., Huang, X., 2023. Carbon distribution and multi-criteria decision analysis of flexible waste biomass smouldering processing technologies. Waste Manag. 167, 183–193. https://doi.org/10.1016/j.wasman.2023.05.038.

Chrysikou, L., Gemenetzis, P., Kouras, A., Manoli, E., Terzi, E., Samara, C., 2008. Distribution of persistent organic pollutants, polycyclic aromatic hydrocarbons and trace elements in soil and vegetation following a large scale landfill fire in northern Greece. Environ. Int. 34, 210–225.

Dabrowska, D., Wojciech, R., Vahid, N., 2023. Causes, types and consequences of municipal waste landfill fires — literature review. Sustainability 1, 13.

Eurostat, E.C., Kotzeva, M., Brandmüller, T., Önnerfors, Å., 2015. Eurostat regional yearbook 2015. Publ. Off. https://doi.org/doi/10.2785/408702.

Fattal, A., Kelly, S., Liu, A., Giurco, D., 2016. Review institute for sustainable futures waste fires in Australia. Cause Concern.

Feng, X., Lu, L., Ouyang, M., Li, J., He, X., 2016. A 3D thermal runaway propagation model for a large format lithium ion battery module. Energy 115, 194–208. https://doi.org/10.1016/j.energy.2016.08.094.

Feng, X., Ren, D., He, X., Ouyang, M., 2020. Mitigating thermal runaway of Lithium-Ion batteries. Joule. https://doi.org/10.1016/j.joule.2020.02.010.

Gabbar, H.A., Othman, A.M., Abdussami, M.R., 2021. Review of battery management systems (BMS) development and industrial standards. Technologies 9, 28.

Hu, G., Huang, P., Bai, Z., Wang, Q., Qi, K., 2021. Comprehensively analysis the failure evolution and safety evaluation of automotive lithium ion battery. ETransportation 10, 100140.

Huang, X., Rein, G., 2019. Downward-and-upward spread of smoldering peat Fire. Proc. Combust. Inst. 37, 4025–4033. https://doi.org/10.1016/j.proci.2018.05.125.

Ji, H., Chung, Y.H., Pan, X.H., Hua, M., Shu, C.M., Zhang, L.J., 2021. Study of lithium-ion battery module's external short circuit under different temperatures. J. Therm. Anal. Calor. 144, 1065–1072. https://doi.org/10.1007/s10973-020-09506-0.

Koelsch, F., Fricke, K., Mahler, C., Damanhuri, E., 2005. Stability of landfills-the Bandung dumpsite disaster. : Proc. Sard.

Krause, M.J., Eades, W., Detwiler, N., Marro, D., Schwarber, A., Tolaymat, T., 2023. Assessing moisture contributions from precipitation, waste, and leachate for active municipal solid waste landfills. J. Environ. Manag. 344, 118443.

Lammer, M., Königseder, A., Hacker, V., 2017. Holistic methodology for characterisation of the thermally induced failure of commercially available 18650 lithium ion cells. RSC Adv. 7, 24425–24429.

Li, Y., Zhang, N., Jiang, L., Wei, Z., Zhang, Y., Yu, Y., Song, L., Wang, L., Duan, Q., Sun, J., Wang, Q., 2024. Assessment of the complete chain evolution process of LIBs from micro internal short circuit failure to thermal runaway under mechanical abuse conditions. Process Saf. Environ. Prot. 185, 296–306. https://doi.org/10.1016/j.psep.2024.03.033.

Liamsanguan, C., Gheewala, S.H., 2008. The holistic impact of integrated solid waste management on greenhouse gas emissions in Phuket. J. Clean. Prod. 16, 1865–1871.

Lin, S., Cheung, Y.K., Xiao, Y., Huang, X., 2020. Can rain suppress smoldering peat fire? Sci. Total Environ. 727, 138468. https://doi.org/10.1016/j.scitotenv.2020.138468.

Lin, S., Huang, X., 2021. Quenching of smoldering: effect of wall cooling on extinction. Proc. Combust. Inst. 38, 5015–5022.

Lin, S., Liu, Y., Huang, X., 2021. Climate-induced Arctic-boreal peatland fire and carbon loss in the 21st century. Sci. Total Environ. 796, 148924. https://doi.org/10.1016/j.scitotenv.2021.148924.

Liu, Y., Niu, H., Liu, J., Huang, X., 2022. Layer-to-layer thermal runaway propagation of open-circuit cylindrical li-ion batteries: effect of ambient pressure. J. Energy Storage 55, 105709. https://doi.org/10.1016/j.est.2022.105709.

Liu, Y., Sun, P., Lin, S., Niu, H., Huang, X., 2020. Self-heating ignition of open-circuit cylindrical Li-ion battery pile: towards fire-safe storage and transport. J. Energy Storage 32, 101842. https://doi.org/10.1016/j.est.2020.101842.

Liu, Y., Zhang, L., Huang, Xianjia, Hao, M., Huang, Xinyan, 2024. Laser-induced thermal runaway dynamics of cylindrical lithium-ion battery. J. Energy Storage 86, 111337. https://doi.org/10.1016/j.est.2024.111337.

Lyon, R.E., Walters, R.N., 2016. Energetics of lithium ion battery failure. J. Hazard. Mater. 318, 164–172.

Makarichi, L., Jutidamrongphan, W., Techato, K., 2018. The evolution of waste-to-energy incineration: a review. Renew. Sustain. Energy Rev. 91, 812–821.
Maleki, H., Howard, J.N., 2009. Internal short circuit in Li-ion cells. J. Power Sources 191, 568–574. https://doi.org/10.1016/j.jpowsour.2009.02.070.
Masalegooyan, Z., Piadeh, F., Behzadian, K., 2022. A comprehensive framework for risk probability assessment of landfill fire incidents using fuzzy fault tree analysis. Process Saf. Environ. Prot. 163, 679–693. https://doi.org/10.1016/j.psep.2022.05.064.
Milosevic, L.T., Mihajlovic, E.R., Djordjevic, A.V., Protic, M.Z., Ristic, D.P., 2018. Identification of fire hazards due to landfill gas generation and emission. Pol. J. Environ. Stud. 27.
Mor, S., Ravindra, K., 2023. Municipal solid waste landfills in lower- and middle-income countries: environmental impacts, challenges and sustainable management practices. Process Saf. Environ. Prot. 174, 510–530. https://doi.org/10.1016/j.psep.2023.04.014.
Øygard, J.K., Måge, A., Gjengedal, E., 2004. Estimation of the mass-balance of selected metals in four sanitary landfills in Western Norway, with emphasis on the heavy metal content of the deposited waste and the leachate. Water Res. 38, 2851–2858.
Qin, Y., Musa, D.N.S., Lin, S., Huang, X., 2022. Deep peat fire persistently smouldering for weeks: a laboratory demonstration. Int. J. Wildl. Fire 32, 86–98. https://doi.org/10.1071/wf22143.
Rein, G., 2013. Smouldering fires and natural fuels. In: Belcher, C.M. (Ed.), Fire Phenomena in the Earth System. An Interdisciplinary Approach to Fire Science, pp. 15–34.
Saanich News Staff, 2023. Smouldering battery nearly causes Saanich landfill fire [WWW Document]. VICTORIA NEWS. URL ⟨https://www.vicnews.com/local-news/smouldering-battery-nearly-causes-saanich-landfill-fire-662074?utm_source=chatgpt.com⟩.
SARET Research Team, 2023. Lithium-Ion Battery Incidents 2022-2023.
Scholten, R.C., Jandt, R., Miller, E.A., Rogers, B.M., Veraverbeke, S., 2021. Overwintering fires in boreal forests. Nature 593, 399–404. https://doi.org/10.1038/s41586-021-03437-y.
Seidelt, S., Müller-Hagedorn, M., Bockhorn, H., 2006. Description of tire pyrolysis by thermal degradation behaviour of main components. J. Anal. Appl. Pyrolysis 75, 11–18.
Song, Z., Huang, X., Kuenzer, C., Zhu, H., Jiang, J., Pan, X., Zhong, X., 2020. Chimney effect induced by smoldering fire in a U-shaped porous channel: a governing mechanism of the persistent underground coal fires. Process Saf. Environ. Prot. 136, 136–147. https://doi.org/10.1016/j.psep.2020.01.029.
Terazono, A., Oguchi, M., Akiyama, H., Tomozawa, H., Hagiwara, T., Nakayama, J., 2024. Resources, Conservation & Recycling Ignition and fire-related incidents caused by lithium-ion batteries in waste treatment facilities in Japan and countermeasures. Resour. Conserv. Recycl. 202, 107398. https://doi.org/10.1016/j.resconrec.2023.107398.
Themelis, N.J., Ulloa, P.A., 2007. Methane generation in landfills. Renew. Energy 32, 1243–1257.
Wang, Y., Feng, X., Huang, W., He, X., Wang, L., Ouyang, M., 2023. Challenges and opportunities to mitigate the catastrophic thermal runaway of high-energy batteries. Adv. Energy Mater. 13, 2203841.
Wang, Q., Ping, P., Zhao, X., Chu, G., Sun, J., Chen, C., 2012. Thermal runaway caused fire and explosion of lithium ion battery. J. Power Sources 208, 210–224. https://doi.org/10.1016/j.jpowsour.2012.02.038.
Weichenthal, S., Van Rijswijk, D., Kulka, R., You, H., Van Ryswyk, K., Willey, J., Dugandzic, R., Sutcliffe, R., Moulton, J., Baike, M., 2015. The impact of a landfill fire on ambient air quality in the north: a case study in Iqaluit, Canada. Environ. Res. 142, 46–50.
Zhang, L., Liu, Y., Huang, X., 2024a. Dynamic thermal runaway evolution of Li-ion battery during nail penetration. Int. J. Heat. Mass Transf. 233. https://doi.org/10.1016/j.ijheatmasstransfer.2024.126020.
Zhang, Y., Shu, Y., Qin, Y., Chen, Y., Lin, S., Huang, X., Zhou, M., 2024b. Resurfacing of underground peat fire: smouldering transition to flaming wildfire on litter surface. Int. J. Wildl. Fire 33, WF23128. https://doi.org/10.1071/WF23128.
Zhao, T., Chae, S., Choi, Y., 2024. A review on recycling of waste lead-acid batteries. J. Phys. Conf. Ser. 2738, 6362–6395. https://doi.org/10.1088/1742-6596/2738/1/012019.
Zhu, N., Wang, X., Chen, M., Huang, Q., Ding, C., Wang, J., 2023. Study on the combustion behaviors and thermal stability of aging lithium-ion batteries with different states of charge at low pressure. Process Saf. Environ. Prot. 174, 391–402. https://doi.org/10.1016/j.psep.2023.04.016.